

Stereochemistry-controlled mechanical properties and degradation in 3D-printable photosets

Khalfa, Anissa; Becker, Matthew L; Dove, Andrew

DOI:

[10.1021/jacs.1c06960](https://doi.org/10.1021/jacs.1c06960)

License:

Creative Commons: Attribution-NonCommercial-NoDerivs (CC BY-NC-ND)

Document Version

Publisher's PDF, also known as Version of record

Citation for published version (Harvard):

Khalfa, A, Becker, ML & Dove, A 2021, 'Stereochemistry-controlled mechanical properties and degradation in 3D-printable photosets', *Journal of the American Chemical Society*. <https://doi.org/10.1021/jacs.1c06960>

[Link to publication on Research at Birmingham portal](#)

General rights

Unless a licence is specified above, all rights (including copyright and moral rights) in this document are retained by the authors and/or the copyright holders. The express permission of the copyright holder must be obtained for any use of this material other than for purposes permitted by law.

- Users may freely distribute the URL that is used to identify this publication.
- Users may download and/or print one copy of the publication from the University of Birmingham research portal for the purpose of private study or non-commercial research.
- User may use extracts from the document in line with the concept of 'fair dealing' under the Copyright, Designs and Patents Act 1988 (?)
- Users may not further distribute the material nor use it for the purposes of commercial gain.

Where a licence is displayed above, please note the terms and conditions of the licence govern your use of this document.

When citing, please reference the published version.

Take down policy

While the University of Birmingham exercises care and attention in making items available there are rare occasions when an item has been uploaded in error or has been deemed to be commercially or otherwise sensitive.

If you believe that this is the case for this document, please contact UBIRA@lists.bham.ac.uk providing details and we will remove access to the work immediately and investigate.

Stereochemistry-Controlled Mechanical Properties and Degradation in 3D-Printable Photosets

Anissa L. Khalfa, Matthew L. Becker, and Andrew P. Dove*



Cite This: <https://doi.org/10.1021/jacs.1c06960>



Read Online

ACCESS |



Metrics & More

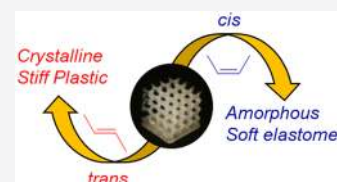


Article Recommendations



Supporting Information

ABSTRACT: Stereochemistry provides an appealing handle by which to control the properties of small molecules and polymers. While it is established that stereochemistry in linear polymers affects their bulk mechanical properties, the application of this concept to photocurable networks could allow for resins that can accommodate the increasing demand for mechanically diverse materials without the need to significantly change their formulation. Herein, we exploit *cis* and *trans* stereochemistry in pre-resin oligomers to create photoset materials with mechanical properties and degradation rates that are controlled by their stereochemistry and molecular weight. Both the synthesis of stereopure (*cis* or *trans*) acrylate-terminated pre-polymers and the subsequent UV-triggered cross-linking occurred with a retention of stereochemistry, close to 100%. The stereochemistry of a 4 kDa oligomer within the resin enabled the tuning of the formulation to either a fast eroding, soft *cis* elastomer or a stiff *trans* plastic that is more resistant to degradation. These results demonstrate that stereochemistry is a powerful tool to modify the stiffness, toughness, and degradability of high-resolution, three-dimensional printed scaffolds from the same formulated ratio of components.



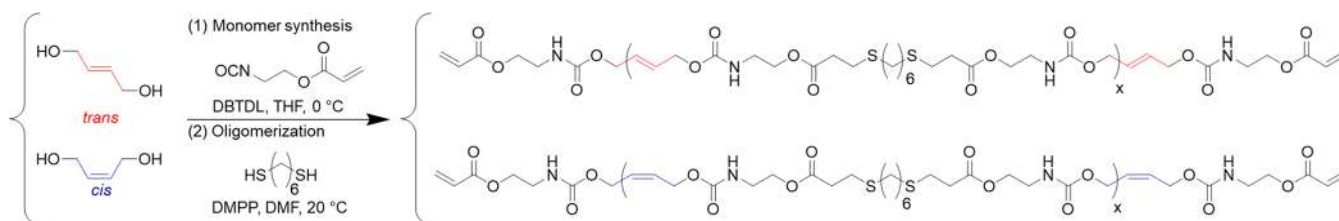
INTRODUCTION

Stereochemistry has been successfully used as a tool to access a broad spectrum of mechanical properties in thermoplastics, but it has not received as much attention within polymer networks.¹ Within the diverse array of polymer networks, photoset materials are appealing on account of the ability to exert spatiotemporal control over the curing process. While there remains a wide range of applications for photoset materials, three-dimensional (3D) printing constitutes an appealing alternative to more traditional material processing, as it allows the rapid production of customizable highly intricate designs, while remaining low cost. As such, it finds applications ranging from consumer products to medical devices.² While there is an ever-increasing variety of techniques available, digital light processing (DLP)-based photochemical printing stands apart in performance by offering micron-scale resolution as well as unprecedented accuracy and speed.^{3,4} Until recently, photocurable resins that are suitable for DLP largely produced brittle materials, thus limiting the potential applications of the technology.^{5,6} However, advances in photochemical methodology (thiol-ene,^{7,8} addition-fragmentation chain transfer,^{9,10} dual cure network¹¹) and the enhancement of formulations with additives (siloxanes,¹² aliphatic chains,¹³ and inorganic fillers¹⁴) have contributed to the development of resins that result in materials with improved toughness and ductility.^{15,16} Modifying the mechanical properties within photosets, however, commonly requires significant changes to the chemical structure of the network (e.g., monomer/oligomer substitution) or its cross-linking density, which inevitably result in altering the printability of the resin without a further adjustment of either the formulation, the printing parameters, or the equipment.^{12,17}

Most commonly, optical stereoisomers with a chiral center on the polymer backbone (i.e., in polypropylene or polylactide) have been studied. However, *cis/trans* isomerism of double bonds within polymer backbones also provides a powerful method by which to manipulate the polymer properties. This is exemplified in 1,4-polyisoprene, in which the *cis* isomer demonstrates soft and elastomeric properties, while *trans*-1,4-polyisoprene is a stiff plastic because of its greater crystallinity.^{18–20} We postulated that UV-curable photoset materials would allow the production of materials in which the mechanical properties could be tuned by simply changing the stereochemistry within the network-forming components to allow for a more simple formulation of resins that could offer a noticeable benefit of time and labor in resin design and help extend the applicability of photoset materials, including 3D-printed materials using DLP.^{13,21}

The development of synthetic polymers that precisely incorporate *cis/trans* stereochemistry within the polymer backbone has been hampered for decades by the synthetic challenges of creating materials that do not undergo isomerization or unwanted cross-linking.^{22–25} However, advances in polymerization methods have revealed milder reaction conditions, and as such, the preparation of polymers in which the *cis/trans* double bond stereochemistry can be

Received: July 5, 2021

Scheme 1. Oligomer Synthesis^a

^a(1) Monomer synthesis: 1 equiv of 1,4-but-2-enediol (*cis* or *trans*), 2.1 equiv of 2-isocyanatoethyl acrylate, 0.2 mol % of dibutyltindilaurate (DBTDL), THF, 0 °C. (2) Oligomer synthesis: 1 equiv of 1,6-hexanedithiol, diacrylate (*cis* or *trans*) in excess, 0.5 equiv of dimethylphenylphosphine (DMPP), DMF (0.25 M).

controlled is more accessible than ever before.¹ To this end, it has been reported that, via the adjustment of solvent polarity and catalyst basicity, the nucleophilic thiol–yne addition of an activated dialkyne with a dithiol yielded stereocontrolled high molecular weight polymers with a *cis* ratio ranging from 32% up to 80% that correlated to mechanical performance.^{26,27}

More recently, we reported a polymerization method based on a nucleophilic thiol–ene addition using a dithiol monomer with a diacrylate monomer that contained a predefined *cis* or *trans* double bond. The reaction was mild enough to preclude the occurrence of isomerization and allowed the retention of stereoregularity in the polymer.²⁸ These reports have been focused on the properties of linear, high molecular weight polymers in which the stereochemistry dictates the extent of crystalline domain formation in the bulk material. However, such an investigation has yet to be undertaken for a cross-linked network. We hypothesized that the use of stereochemistry to leverage mechanical properties of cross-linked photoset networks comprised of short oligomer chains, in which the chain length and cross-linking likely inhibit associations driven by stereochemistry, would in turn offer unique opportunities to streamline the design of photocurable resins with divergent properties. To this end, the development of methods that allow for network formation but do not lead to an isomerization of stereochemically defined groups during the process is important to allow the elucidation of these effects on the mechanical and physical properties of the resulting materials to be understood in a systematic manner.

Herein, we take advantage of the orthogonal reactivity of different alkenes to develop photosets and 3D-printed scaffolds with stereochemically dependent mechanical properties and degradability. Acrylate-terminated stereochemically defined (*cis* and *trans*) poly(ester-urethane) oligomers were obtained from diacrylate monomers with predefined *cis* or *trans* stereochemistry via nucleophilic thiol–Michael addition. The synthesis of the pre-polymer and subsequent network formation occurred without significant isomerization or cross-linking of the in-chain alkenes as proven by ¹H NMR spectroscopic analysis of the depolymerized photosets. Leveraging the *cis/trans* stereochemistry within the network offered excellent control over the mechanical and degradation properties of the resultant 3D structures.

RESULTS AND DISCUSSION

Stereopure unsaturated oligomers were synthesized by a reaction of unsaturated diols (*cis* or *trans*) with the commercially available 2-isocyanatoethyl acrylate in tetrahydrofuran (THF). The diacrylate products were subsequently oligomerized with 1,6-hexanedithiol using a phosphine-

catalyzed thiol–Michael step-growth addition, following a previously reported procedure²⁸ that was modified by using an excess of diacrylate in order to obtain acrylate-terminated oligomers (Scheme 1). A monomer concentration of 0.25 M in dimethylformamide (DMF) was chosen for the oligomer synthesis, since the reaction was rapid at this concentration (30–45 min), yet dilute enough to minimize a premature cross-linking of the formed oligomer. The thiol addition proceeded selectively onto the acrylic double bond β carbon, and no apparent side reactions, such as cross-linking or isomerization, involving the in-chain unsaturation, were detected by ¹H NMR spectroscopy (Supporting Information, Figures S9–S19). The high reactivity of the acrylic double bond suggested that a further photochemical reaction of a resin formulated from these oligomers would result in a selective cross-linking through that bond, leaving the in-chain alkene unreacted, thus retaining stereochemical control over the material properties within the resultant photosets.

Mixing the obtained stereochemically defined oligomers with *N*-methylpyrrolidone (NMP, unreactive diluent) and ethyl(2,4,6-trimethylbenzoyl)phenylphosphine (TPO-L, photoinitiator) in a ratio of 50:50:0.5 wt % allowed the production of distinct *cis* and *trans* photocurable resins. The choice of NMP as an unreactive diluent was critical, as it was found to have a superior solubilization performance to the other diluents examined, which facilitated the formulation of stable resin at ambient temperature. After a UV irradiation (300 < λ < 700 nm, 11 W) and thermal postcuring (120 °C, 24 h), *cis* and *trans* photoset films were obtained. While the in-chain nonpolar alkene bonds were expected to have poor reactivity toward photo-cross-linking, it has been shown previously that they are able to isomerize when exposed to UV irradiation in the presence of a photosensitizer.^{29,30} Thus, prior to mechanical testing, the incidence of isomerization during the curing process was investigated. The monomer design allowed for both construction of the oligomers and network formation through the acrylate, and a depolymerization of the resulting materials through the ester bond that is present in the materials. To this end, *cis* and *trans* films obtained after 20 s or 15 min of UV irradiation and thermal postcuring were degraded by methanolysis of the ester moieties and analyzed by ¹H NMR spectroscopy (Figure 1a).

Focusing on the vinyl region of the ¹H NMR spectra clearly highlights that the *trans* bond geometry is not affected by photocuring. In contrast, exposing the *cis* resin to UV light for 15 min resulted in 36% isomerization of the in-chain double bonds. However, at lower exposure times (20 s), less than 1% of isomerization was observed within the *cis* film (Figure 1b), which did not change after thermal postcuring. A more in-

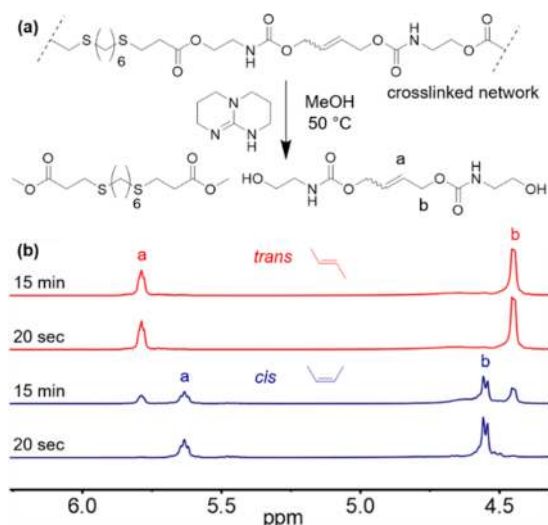


Figure 1. (a) The network is degraded by a transesterification in methanol with triazabicyclodecene (TBD) as a catalyst. The reaction is undertaken at 50 °C and completed in 30 min, when no solid could be observed in the medium. (b) Comparison of ^1H NMR spectra in the vinyl region of the degraded *trans* and *cis* films cured for either 15 min or 20 s. While the irradiation time does not affect the *trans* alkenes, the *cis* alkenes undergo an isomerization when irradiated for 15 min.

depth investigation of this effect using a *cis*-oligomer that had been end-capped with 1-hexanethiol (in order to solely focus on isomerization in the absence of cross-linking) revealed that a maximum of 60% conversion to the *trans* isomer was possible within ca. 10 min and that, without a photoinitiator, no isomerization occurred (Figures S36 and S37). This result has three important implications: (i) the networks are at least 99% stereochemically defined when cured for a short period of time, which means that (ii) a comparison of the mechanical properties of *cis* and *trans* materials will give reliable information about the influence of stereochemistry on bulk properties and (iii) curing the oligomers into a network limits the ability of the oligomers to undergo isomerization. Thus, short exposures to UV light were maintained through the study.

As a result of the low photochemical reactivity of internal alkenes, cross-links were solely formed at the acrylate end groups. Hence, we hypothesized that increasing the molecular weight of the oligomer that the resin is composed from should also impact the mechanical properties. To elucidate both the

impact of the stereochemistry and the oligomer length on the mechanical properties of the network, *cis* and *trans* films were cured from a resin based on stereochemically pure oligomers with a molecular weight of ca. 4 kDa. The resulting films were subjected to uniaxial tensile testing, along with films prepared by cross-linking resins based on oligomers of ~6 and 10 kDa (Figure 2). For resins based on shorter oligomers, a striking difference existed between the tensile profiles of the *cis* and *trans* photoset films. The UV-cured material that contained *trans* oligomers of ~4 kDa exhibited a Young's modulus (E) of 64 MPa, a yield point (σ_y) of ~10 MPa and a strain at 30% elongation at break (ϵ_b) of 98% (Figure 2a). This behavior is typical of a stiff and moderately ductile plastic and is comparable to commercially available acrylic 3D printing resins.³¹ Conversely, the *cis* UV-cured material exhibited a Young's modulus that is 50 times smaller than the *trans* material and displayed no yield point, typical of an elastomeric material. Increasing the oligomer molecular weight within the resins from ca. 4 kDa to ca. 6 kDa led to films that displayed the same response to tensile stress but in which the strain at break increased to reach 300% (Figure 2b). Further increasing the molecular weight of the oligomer to ca. 10 kDa resulted in a resin that, when photocured, exhibited improved ductility and strain at break (647%) for the *trans* material; however, the *cis* material unexpectedly behaved similarly. Thus, the *cis* film only shows a 40% improvement of its strain at break, while diverging from the elastomeric behavior to display plastic deformation (Figure 2c). Consequently, while still distinct, the difference between *cis* and *trans* materials became less prominent when longer oligomeric chains were employed in the resin. With stereochemistry being the only variable between *cis* and *trans* films at a given molecular weight, it is possible to state that it constitutes the basis of the mechanical divergence displayed by the photosets.

We have previously demonstrated that the *cis* and *trans* high molecular weight linear polymer analogues both display a plastic deformation, with the *cis* isomer being the softer and weaker isomer.¹¹ In the networks reported herein, the behavior is more analogous to that previously observed in polyisoprene^{32,33} and polybutadiene.³⁴ In these examples, the *trans* alkene results in linear backbones that are capable of good chain packing which, in turn, promote a high degree of crystallinity within the polymeric structure. Conversely, *cis* alkenes impede the linearity of the backbone and result in a less-ordered structure, reducing the crystallization ability and, consequently, leading to more amorphous materials with soft, elastic properties. We postulate that similar chain-packing

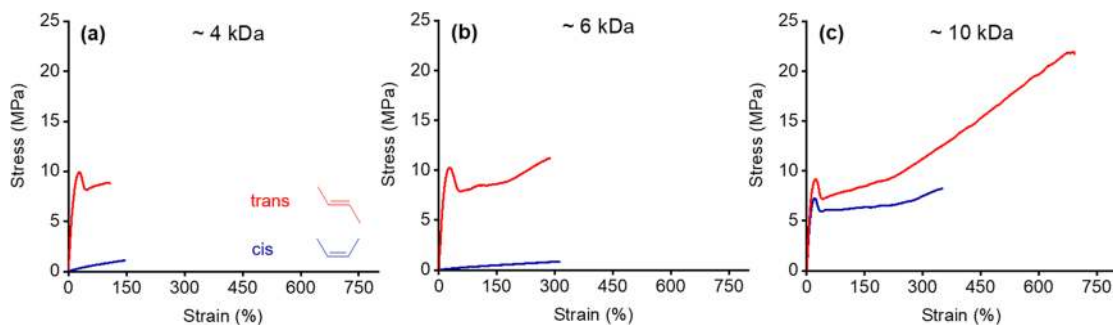


Figure 2. Representative stress–strain curves of (a) a 4.5 kDa *trans* film and a 4.0 kDa *cis* film. (b) 6.1 kDa *trans* film and a 6.1 kDa *cis* film. (c) A 9.7 kDa *trans* film and a 9.7 kDa *cis* film. The molecular weights were determined by ^1H NMR spectroscopy analysis (For details see the Supporting Information—eq 4, Table S2).

reasons explain the change in behavior that we observe here with increasing oligomer molecular weight. The selective cross-linking at the acrylate end group means that an increase of the oligomer chain length is equivalent to an increase of the average molecular weight between cross-links (M_c), which, in turn, induces an overall gain in ductility. The same argument could also explain the unexpected stiffness of the 9.7 kDa *cis* film, as with a higher M_c , the chains have more mobility to organize and the likelihood of crystallization is higher; thus, these chains behave in a more analogous manner to the high molecular weight linear polymers.²⁸ A swelling study conducted on these photosets confirmed the linear relationship between the average molecular weight of the linear oligomer and the cross-linking density (Figure S43).

Conducting differential scanning calorimetry (DSC) analysis on these materials highlighted the expected correlation between mechanical properties and crystallinity within the cross-linked networks (Figure 3). After 2 d of being annealed

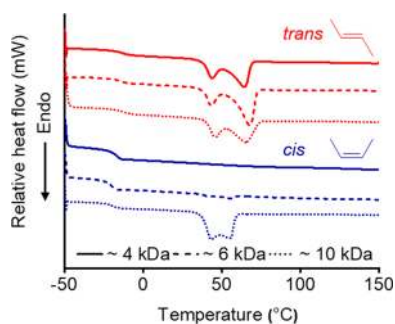


Figure 3. First heating scans of DSC thermograms for *trans* films of 4.5, 6.1, and 10 kDa showing a constant degree of crystallization and *cis* films of 4.0, 6.1, and 10 kDa showing the dependence of the crystallinity with the oligomer chain length.

at room temperature, all *trans* films display two first-order melt transitions (45 and 65 °C) on the first heating scan with a total melting enthalpy (ΔH_m) ranging between 26 and 28 J·g⁻¹. This indicates that, regardless of the oligomer chain length, *trans* films exist as a semicrystalline network. The presence of two melting peaks was observed in the high molar mass linear analogues²⁸ and is typically observed in *trans*-1,4-polyisoprene and isotactic polypropylene, where it is ascribed to the presence of different crystalline domains within the bulk material.^{35,36} Conversely, the *cis* films display melting transitions that are directly related to the oligomer molecular weight. For the 4 kDa *cis* sample, no melting is observed on the

first heating scan, and a melting transition is only barely detectable (ΔH_m of 2.6 J·g⁻¹) on the first heating scan of the 6 kDa *cis* film. However, the 9.7 kDa *cis* film displays a significant (ΔH_m of 25 J·g⁻¹) and broad melting transition from 43 to 56 °C. A re-analysis of the same films by DSC after two weeks and 10 months of being annealed under ambient conditions indicated a discernible increase in the magnitude of the melting transition for the 6 kDa *cis* film, where ΔH_m increases from 2.6 J·g⁻¹ at 2 d to 20 J·g⁻¹ after two weeks of annealing (Figure S41). Consequently, it is possible to conclude that, after 2 d, the *trans* materials are semicrystalline networks independently of their molecular weight, thus explaining their stiff and tough plastic behavior during tensile testing. In the case of *cis* films, however, the crystallization behavior of the network was correlated to the chain length of the oligomeric pre-polymer, as the *cis* film formed from 4 kDa oligomers is amorphous, whereas both the films formed from 6.1 and 9.7 kDa oligomers were semicrystalline. Moreover, the molecular weight of the oligomers within the network also clearly impacted the rate at which the films crystallized. The film formed from 6 kDa oligomers did not change after two weeks of annealing, whereas the film formed from ~10 kDa oligomers only required 2 d to reach its final degree of crystallinity. This highlights why the former still behaves as a soft elastomer after 2 d of annealing, while the latter acts as a stiff plastic.

Calculating the cross-link density from the mechanical properties and swelling data from fully post-cured materials confirmed that, in all cases, the materials derived from oligomers with *trans* double-bond stereochemistry had a higher cross-link density than those with *cis* double-bond stereochemistry. Moreover, this was unaffected by the initial cure time, but the *cis* film cured from the oligomer with the highest molar mass displayed a significantly higher cross-link density (Figure S53). These observations are consistent with the increase in crystallinity observed in the materials and likely are a reflection of both the cross-linking within the network as well as the crystalline domain formation, which would also be expected to hinder swelling and, in turn, the calculated cross-link density.

Resins that contain either *cis* or *trans* oligomers showed physical properties that made them good candidates for stereolithographic 3D printing including a viscosity below 1 Pa·s⁻¹ and a rapid gelation rate (Figures S45 and S46 and Table S8). However, to fully benefit from the high resolution permitted by stereolithography, control over the light penetration depth was required. To this end, Kalsec Durabrite Oleoresin Paprika Extract NS (a common food additive) was

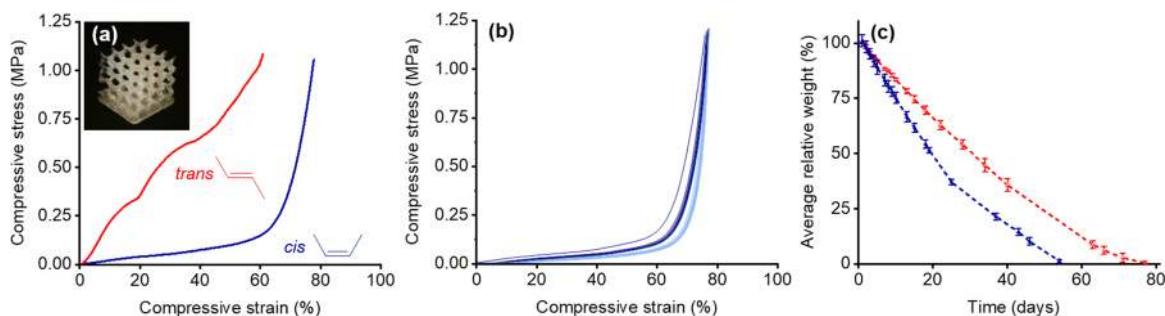


Figure 4. (a) Compressive stress–strain curves of *cis* and *trans* scaffolds, and a picture of a 3D-printed scaffold. (b) Stress and strain obtained from the cyclic compression of a *cis* scaffold submitted to stress up to ~1.15 MPa for 10 cycles. The loading cycles are represented in dark blue, and the relaxation cycles are in light blue. (c) Degradation curves of *cis* and *trans* photosets.

added to the original resin formulation at a ratio of 0.5 wt % to act as a photoinhibitor and control the light scattering and penetration depth (Figure S52).³⁷ An individual stepwise adjustment of the printing parameters demonstrated that an irradiation of 50 μm thick layers for 25 s resulted in the highest printing accuracy for both *cis* and *trans* resins. As such, high-resolution scaffolds of 6 mm in height were obtained by using these settings (Figure 4a, inset). Notably, despite requiring up to 50 wt % NMP in the resin formulation to reduce its viscosity such that it was suitable for printing, the 3D printed parts shrunk in a homogeneous manner that did not affect the integrity of the structure.

Uniaxial compressive tests were conducted on these scaffolds to determine if *cis* and *trans* stereochemistry could influence the mechanical properties of 3D-printed structures (Figure 4a). Since compression of 3D materials does not usually result in clear fracture patterns at failure,³⁸ the compression tests were only conducted up to 50 N force (1 MPa stress) to not cause irreversible damage to the scaffolds. When we corroborated observations for the *cis/trans* photostat films, the stereochemistry within the 3D-printed scaffolds also had a strong influence on their mechanical properties. The *trans* scaffold demonstrated a plastic deformation along with a compressive Young's modulus (E_c) of ~ 2.4 MPa, whereas the *cis* scaffold deformation corresponded to an elastic material with an E_c 20 times smaller. The elastic properties of the *cis* scaffold were further investigated by running cyclic compressive tests. As typically observed in elastomeric materials, softening occurred after the first loading–unloading cycle, and the stabilization of the stress–strain curve occurred after three or four cycles (Figure 4b).^{39–42} The unloading of stress from the material shows a hysteresis of $28 \text{ kJ}\cdot\text{m}^{-3}$ and an average residual strain of 4.5%, which is indicative of a very good recovery capacity of the *cis* material after deformation (Figure 4b). The thermal properties of both scaffolds, according to DSC analysis, also align with their mechanical behavior, where the material is more crystalline than the *cis* structure (Figure S42). After mechanical testing, an elastic *cis* scaffold was degraded and analyzed by ^1H NMR spectroscopy to assess if any isomerization had occurred during the 3D-printing step. Similarly to the photostat materials, the isomerization occurring from irradiation during the 3D printing was negligible (2%, Figure S32).

As crystallinity is known to affect the degradation properties of materials, the hydrolytic degradation of *cis* and *trans* materials was examined under accelerated conditions in order to observe degradation within a reasonable time period.⁴³ Thin cylinders were fabricated from the *cis* and *trans* 3D-printing resins and degraded in an aqueous solution of 1 M NaOH at 37 °C (Figure 4c). The *trans* material fully degraded after 77 d, while the *cis* material only required 54 d to reach the same point. Furthermore, both materials seem to undergo a linear degradation, which is usually representative of a surface erosion mechanism⁴⁴ as opposed to bulk, uncontrolled degradation.

CONCLUSION

By incorporating acrylate-terminated stereopure pre-polymers into UV active resins, stereochemically defined (*cis* and *trans*) poly(ester urethane) photostats have been obtained. The increased reactivity of the acrylic double bonds enabled both the oligomer synthesis and photoinitiated cross-linking of the materials with retention of the stereochemically defined double bond within the material that can dictate the final mechanical

properties. Low exposure times were required to prevent isomerization of the in-chain double bonds. The mechanical properties of the thermosets were dependent on the average molecular weight of the pre-polymer for both materials. A significant change in behavior resulted from increasing the oligomer length from ~ 4 , to 6, to ~ 10 kDa in the resin that formed the *cis* material. We attribute this change in behavior, from elastic to plastic, to the increase in the average molecular weight between cross-links—allowing for greater chain flexibility to, in turn, favor the crystallization of the network as seen in high molecular weight linear polymers of the same chemistry. It is well-established that the polymer length and mechanical properties (such as ductility) have a strong interdependence; however, the presented stereochemical control of bulk properties is unmatched for existing photostat materials. Finally, the addition of a photoinhibitor to the formulation rendered the resins suitable for 3D printing and allowed the preparation of high-resolution 3D scaffolds with stereochemically tunable mechanical and degradable properties. Together, these results enable the control of the mechanical and/or degradation properties of 3D-printed materials by only leveraging the stereochemistry of the pre-polymer without the need of further formulation adaptations. This novel method of controlling the bulk properties of materials produced via additive manufacturing could be envisioned as a straightforward technique to access a diverse library of materials using a single formulation. Furthermore, it could also be useful in the creation of graded multimaterials by using advanced DLP, direct ink write (DIW), or inkjet printing methods, in which the *cis/trans* content could be rationally exploited across the physical material structure.

ASSOCIATED CONTENT

Supporting Information

The Supporting Information is available free of charge at <https://pubs.acs.org/doi/10.1021/jacs.1c06960>.

Protocols and further experimental details (PDF)

AUTHOR INFORMATION

Corresponding Author

Andrew P. Dove – School of Chemistry, University of Birmingham, Edgbaston B15 2TT, U.K.; orcid.org/0000-0001-8208-9309; Email: A.Dove@bham.ac.uk

Authors

Anissa L. Khalfa – School of Chemistry, University of Birmingham, Edgbaston B15 2TT, U.K.

Matthew L. Becker – Department of Chemistry, Mechanical Engineering and Materials Science, Biomedical Engineering and Orthopedic Surgery, Duke University, Durham, North Carolina 20899, United States; orcid.org/0000-0003-4089-6916

Complete contact information is available at: <https://pubs.acs.org/doi/10.1021/jacs.1c06960>

Author Contributions

All authors have given approval to the final version of the manuscript.

Notes

The authors declare no competing financial interest.

ACKNOWLEDGMENTS

A.L.K. thanks the University of Birmingham for funding to support her studies. M.L.B. is grateful to the Biomaterials Division of the National Science Foundation for funding portions of this work (DMR-1507420) and A.P.D. acknowledges that this project has received funding from the European Research Council (ERC) under the European Union's Horizon 2020 research and innovation programme under grant agreement 681559.

REFERENCES

- (1) Worch, J. C.; Prydderch, H.; Jimaja, S.; Bexis, P.; Becker, M. L.; Dove, A. P. Stereochemical enhancement of polymer properties. *Nat. Rev. Chem.* **2019**, *3*, 514–535.
- (2) Ligon, S. C.; Liska, R.; Stampfl, J.; Gurr, M.; Mühlaupt, R. Polymers for 3D Printing and Customized Additive Manufacturing. *Chem. Rev.* **2017**, *117*, 10212–10290.
- (3) Yao, L.; Hu, P.; Wu, Z.; Liu, W.; Lv, Q.; Nie, Z.; Zhengdi, H. Comparison of accuracy and precision of various types of photocuring printing technology. *J. Phys.: Conf. Ser.* **2020**, *1549*, 032151.
- (4) Zhang, J.; Hu, Q.; Wang, S.; Tao, J.; Gou, M. Digital Light Processing Based Three-dimensional Printing for Medical Applications. *Int J Bioprint* **2019**, *6*, 242–242.
- (5) Bagheri, A.; Jin, J. Photopolymerization in 3D Printing. *ACS Appl. Polym. Mater.* **2019**, *1*, 593–611.
- (6) Zhang, J.; Xiao, P. 3D printing of photopolymers. *Polym. Chem.* **2018**, *9*, 1530–1540.
- (7) Chen, L.; Wu, Q.; Wei, G.; Liu, R.; Li, Z. Highly stable thiol-ene systems: from their structure–property relationship to DLP 3D printing. *J. Mater. Chem. C* **2018**, *6*, 11561–11568.
- (8) Sycks, D. G.; Wu, T.; Park, H. S.; Gall, K. Tough, stable spiroacetal thiol-ene resin for 3D printing. *J. Appl. Polym. Sci.* **2018**, *135*, 46259.
- (9) Gorsche, C.; Seidler, K.; Knaack, P.; Dorfinger, P.; Koch, T.; Stampfl, J.; Moszner, N.; Liska, R. Rapid formation of regulated methacrylate networks yielding tough materials for lithography-based 3D printing. *Polym. Chem.* **2016**, *7*, 2009–2014.
- (10) Zhang, Z.; Corrigan, N.; Bagheri, A.; Jin, J.; Boyer, C. A Versatile 3D and 4D Printing System through Photocontrolled RAFT Polymerization. *Angew. Chem., Int. Ed.* **2019**, *58*, 17954–17963.
- (11) Xiao, P.; Dumur, F.; Frigoli, M.; Tehfe, M.-A.; Graff, B.; Fouassier, J. P.; Gimes, D.; Lalevée, J. Naphthalimide based methacrylated photoinitiators in radical and cationic photopolymerization under visible light. *Polym. Chem.* **2013**, *4*, 5440–5448.
- (12) Palaganas, J.; de Leon, A. C.; Mangadla, J.; Palaganas, N.; Mael, A.; Lee, Y. J.; Lai, H. Y.; Advincula, R. Facile Preparation of Photocurable Siloxane Composite for 3D Printing. *Macromol. Mater. Eng.* **2017**, *302*, 1600477.
- (13) Patel, D. K.; Sakhaei, A. H.; Layani, M.; Zhang, B.; Ge, Q.; Magdassi, S. Highly Stretchable and UV Curable Elastomers for Digital Light Processing Based 3D Printing. *Adv. Mater.* **2017**, *29*, 1606000.
- (14) Liu, Y.; Lin, Y.; Jiao, T.; Lu, G.; Liu, J. Photocurable modification of inorganic fillers and their application in photopolymers for 3D printing. *Polym. Chem.* **2019**, *10*, 6350–6359.
- (15) Zhou, L.-Y.; Fu, J.; He, Y. A Review of 3D Printing Technologies for Soft Polymer Materials. *Adv. Funct. Mater.* **2020**, *30*, 2000187.
- (16) Truby, R. L.; Lewis, J. A. Printing soft matter in three dimensions. *Nature* **2016**, *540* (7633), 371–378.
- (17) Thrasher, C. J.; Schwartz, J. J.; Boydston, A. J. Modular Elastomer Photoresins for Digital Light Processing Additive Manufacturing. *ACS Appl. Mater. Interfaces* **2017**, *9*, 39708–39716.
- (18) Kent, E. G.; Swinney, F. B. Properties and applications of trans-1,4-polyisoprene. *Ind. Eng. Chem. Prod. Res. Dev.* **1966**, *5*, 134–138.
- (19) Ebewele, R. O. Chemical Bonding and Polymer Structure. In *Polymer science and technology*; CRC Press: New York, 2000.
- (20) Kuzma, L. J. Polybutadiene and Polyisoprene Rubbers. In *Rubber Technology*; Morton, M., Ed.; Springer: Boston, MA, 1987.
- (21) Borrello, J.; Nasser, P.; Iatridis, J. C.; Costa, K. D. 3D printing a mechanically-tunable acrylate resin on a commercial DLP-SLA printer. *Addit. Manuf.* **2018**, *23*, 374–380.
- (22) Yu, Y.; Wei, Z.; Leng, X.; Li, Y. Facile preparation of stereochemistry-controllable biobased poly(butylene maleate-co-butylene fumarate) unsaturated copolyesters: a chemoselective polymer platform for versatile functionalization via aza-Michael addition. *Polym. Chem.* **2018**, *9*, 5426–5441.
- (23) Timmer, M. D.; Ambrose, C. G.; Mikos, A. G. In vitro degradation of polymeric networks of poly(propylene fumarate) and the crosslinking macromer poly(propylene fumarate)-diacrylate. *Biomaterials* **2003**, *24*, 571–577.
- (24) Walker, J. M.; Bodamer, E.; Krebs, O.; Luo, Y.; Kleinfehn, A.; Becker, M. L.; Dean, D. Effect of Chemical and Physical Properties on the In Vitro Degradation of 3D Printed High Resolution Poly(propylene fumarate) Scaffolds. *Biomacromolecules* **2017**, *18*, 1419–1425.
- (25) Lewandrowski, K.-U.; Gresser, J. D.; Wise, D. L.; White, R. L.; Trantolo, D. J. Osteoconductivity of an injectable and bioresorbable poly(propylene glycol-co-fumaric acid) bone cement. *Biomaterials* **2000**, *21*, 293–298.
- (26) Bell, C. A.; Yu, J.; Barker, I. A.; Truong, V. X.; Cao, Z.; Dobrinyin, A. V.; Becker, M. L.; Dove, A. P. Independent control of elastomer properties through stereocontrolled synthesis. *Angew. Chem., Int. Ed.* **2016**, *55*, 13076–13080.
- (27) Worch, J. C.; Weems, A. C.; Yu, J.; Arno, M. C.; Wilks, T. R.; Huckstepp, R. T. R.; O'Reilly, R. K.; Becker, M. L.; Dove, A. P. Elastomeric polyamide biomaterials with stereochemically tuneable mechanical properties and shape memory. *Nat. Commun.* **2020**, *11*, 3250.
- (28) Stubbs, C. J.; Worch, J. C.; Prydderch, H.; Becker, M. L.; Dove, A. P. Unsaturated Poly(ester-urethanes) with Stereochemically Dependent Thermomechanical Properties. *Macromolecules* **2020**, *53*, 174–181.
- (29) Golub, M. A. Photochemistry of unsaturated polymers. In *Chemical Transformations of Polymers*; Rado, R., Ed.; Butterworth-Heinemann, 1972; pp 105–117.
- (30) Schulz, D. N.; Turner, S. R.; Golub, M. A. Recent Advances in the Chemical Modification of Unsaturated Polymers. *Rubber Chem. Technol.* **1982**, *55*, 809–859.
- (31) Lovo, J. F. P.; Camargo, I. L. d.; Erbereli, R.; Morais, M. M.; Fortulan, C. A. Vat Photopolymerization Additive Manufacturing Resins: Analysis and Case Study. *Mater. Res.* **2020**, *23*. DOI: 10.1590/1980-5373-mr-2020-0010
- (32) Baboo, M.; Dixit, M.; Sharma, K.; Saxena, N. S. Mechanical and thermal characterization of cis-polyisoprene and trans-polyisoprene blends. *Polym. Bull.* **2011**, *66*, 661–672.
- (33) Bhowmick, A. K.; Kuo, C. C.; Manzur, A.; MacArthur, A.; McIntyre, D. Properties of cis-and trans-polyisoprene blends. *J. Macromol. Sci., Part B: Phys.* **1986**, *25*, 283–306.
- (34) Short, J. N.; Thornton, V.; Kraus, G. Effect of Cis-Trans Ratio on the Physical Properties of 1,4 Polybutadienes. *Rubber Chem. Technol.* **1957**, *30*, 1118–1141.
- (35) Passingham, C.; Hendra, P. J.; Cudby, M. E. A.; Zichy, V.; Weller, M. The re-evaluation of multiple peaks in the DSC melting endotherm of isotactic polypropylene. *Eur. Polym. J.* **1990**, *26*, 631–638.
- (36) Cooper, W.; Vaughan, G. Crystallization of gutta percha and synthetic trans-1,4-Polyisoprenes. *Polymer* **1963**, *4*, 329–340.
- (37) Barker, I. A.; Ablett, M. P.; Gilbert, H. T.; Leigh, S. J.; Covington, J. A.; Hoyland, J. A.; Richardson, S. M.; Dove, A. P. A microstereolithography resin based on thiol-ene chemistry: towards biocompatible 3D extracellular constructs for tissue engineering. *Biomater. Sci.* **2014**, *2*, 472–475.
- (38) *Standard Test Method for Compressive Properties of Rigid Plastics*; ASTM International: West Conshohocken, PA, 2015.

- (39) Diani, J.; Fayolle, B.; Gilormini, P. A review on the Mullins effect. *Eur. Polym. J.* **2009**, *45*, 601–612.
- (40) Bergström, J. S.; Boyce, M. C. Constitutive modeling of the large strain time-dependent behavior of elastomers. *J. Mech. Phys. Solids* **1998**, *46*, 931–954.
- (41) Mullins, L. Softening of rubber by deformation. *Rubber Chem. Technol.* **1969**, *42*, 339–362.
- (42) Drozdov, A. D.; Dorfmann, A. Stress–strain relations in finite viscoelastoplasticity of rigid-rod networks: applications to the Mullins effect. *Continuum Mech. Thermodyn.* **2001**, *13*, 183–205.
- (43) Göpferich, A. Mechanisms of polymer degradation and erosion. *Biomaterials* **1996**, *17*, 103–114.
- (44) Laycock, B.; Nikolić, M.; Colwell, J. M.; Gauthier, E.; Halley, P.; Bottle, S.; George, G. Lifetime prediction of biodegradable polymers. *Prog. Polym. Sci.* **2017**, *71*, 144–189.